Table S2, related to Figure 1: Malignant tissues sequenced per case in paired cohort**.**

	TISSUE							
DONOR	PANCREAS	LIVER	LYMPH NODE	ADRENAL GLAND	LUNG	DIAPHRAGM	HEART	OMENTUM
Paired Primaries & Metastases								
PCSI0378	1	1	1					
PCSI0380	1	1	1					
PCSI0387	1	1						
PCSI0388	1	1						
PCSI0407	1	1	1					
PCSI0410		1	1	1	2	1	1	1
PCSI0612	1			1				
PCSI0633	1	1						
PCSI0652	1	1						
PCSI0654		2[#]						
PCSI0662		2[#]						
PCSI0665		2[#]						
Paired Primary-Primaries								
PCSI0102	2 [a,c]							
PCSI0357	3 [a]							
PCSI0631	2 [a,c]							
PCSI0635	2 [a,c]							
PCSI0636	2 [b,c]							
PCSI0705	3 [b]							
PCSI0683	2 [b]							

[#] = liver metastases pairs, collected before and after chemotherapy, [a] = metachronous, [b] = synchronous, [c] = targeted panel sequencing

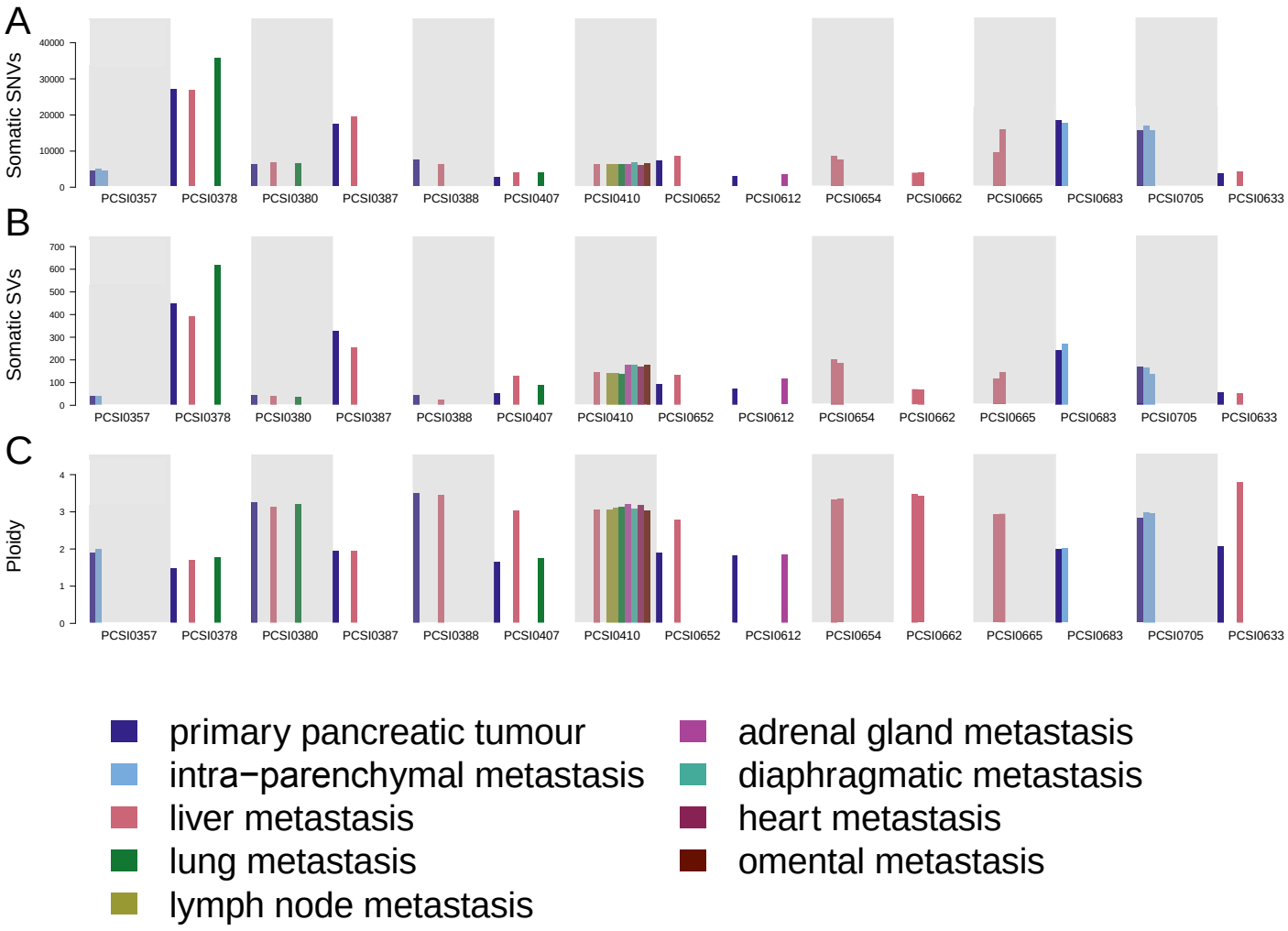

Figure S1: Related to Figure 2. (A-C) Number of point mutations (A), chromosomal rearrangements (B) and tumor ploidy (C) in paired primaries and metastases.

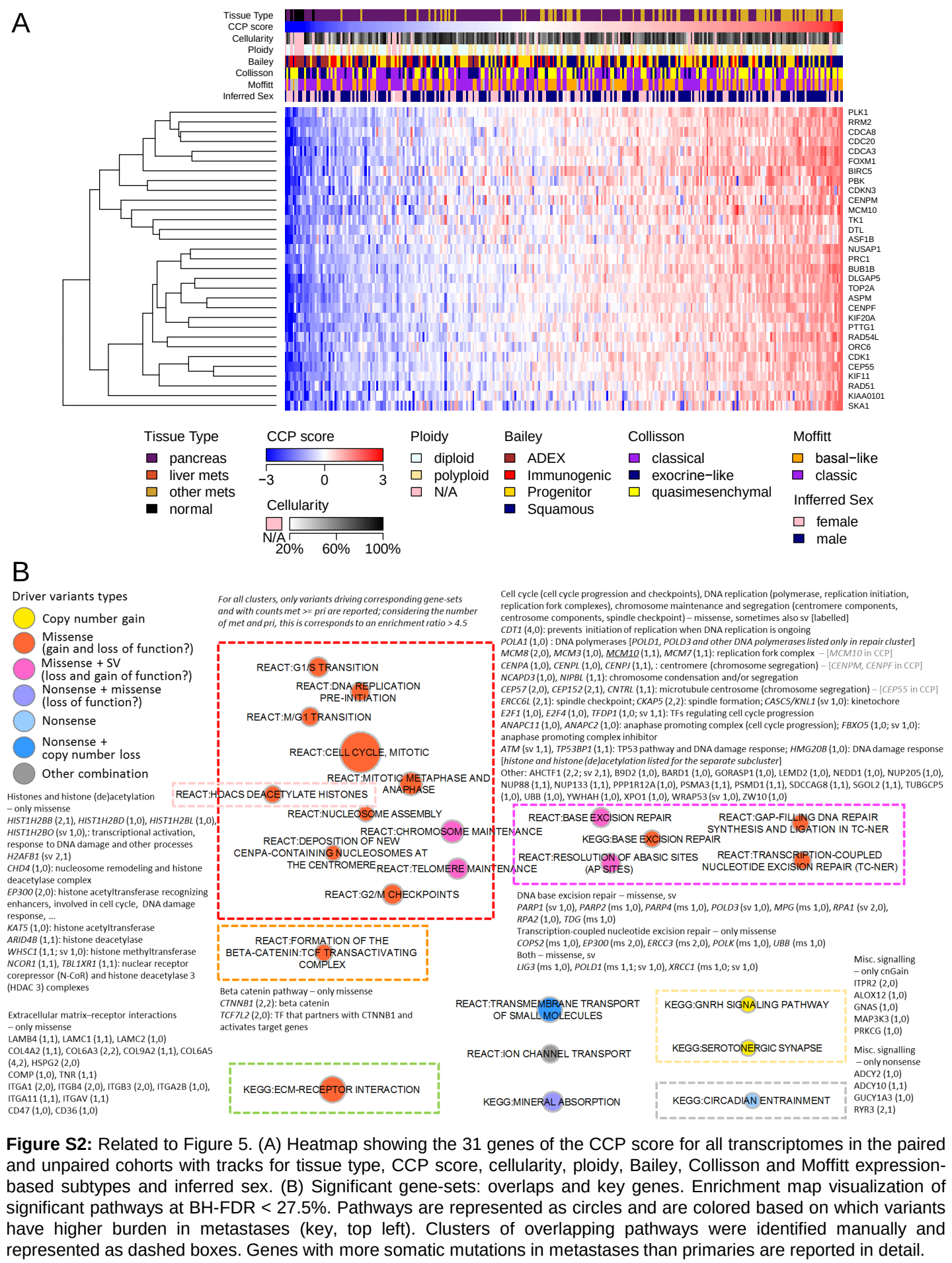

Figure S2: Related to Figure 5. (A) Heatmap showing the 31 genes of the CCP score for all transcriptomes in the paired and unpaired cohorts with tracks for tissue type, CCP score, cellularity, ploidy, Bailey, Collisson and Moffitt expression-based subtypes and inferred sex. (B) Significant gene-sets: overlaps and key genes. Enrichment map visualization of significant pathways at BH-FDR < 27.5%. Pathways are represented as circles and are colored based on which variants have higher burden in metastases (key, top left). Clusters of overlapping pathways were identified manually and represented as dashed boxes. Genes with more somatic mutations in metastases than primaries are reported in detail.

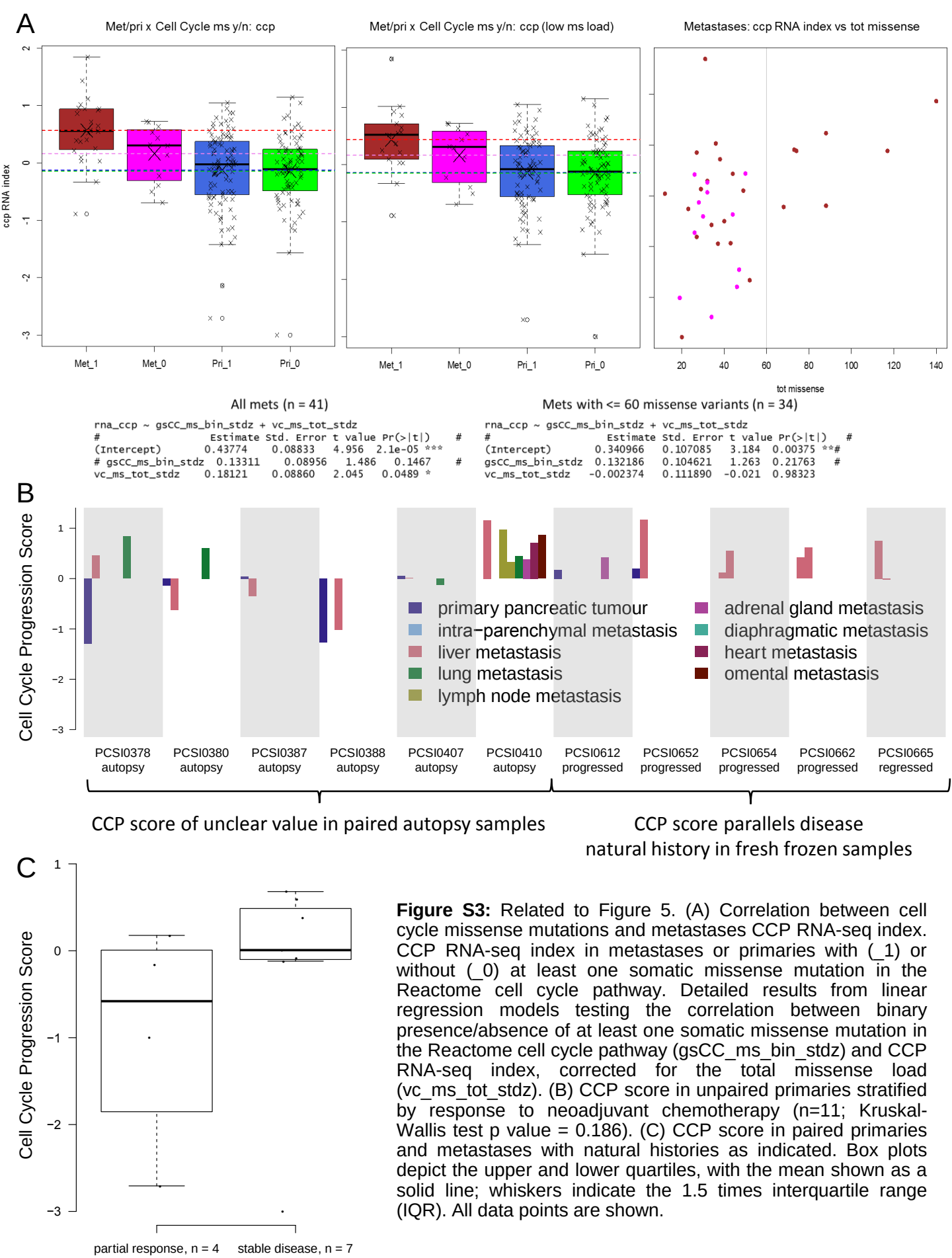

Figure S3: Related to Figure 5. (A) Correlation between cell cycle missense mutations and metastases CCP RNA-seq index. CCP RNA-seq index in metastases or primaries with (_1) or without (_0) at least one somatic missense mutation in the Reactome cell cycle pathway. Detailed results from linear regression models testing the correlation between binary presence/absence of at least one somatic missense mutation in the Reactome cell cycle pathway (gsCC_ms_bin_stdz) and CCP RNA-seq index, corrected for the total missense load (vc_ms_tot_stdz). (B) CCP score in unpaired primaries stratified by response to neoadjuvant chemotherapy (n=11; Kruskal-Wallis test p value = 0.186). (C) CCP score in paired primaries and metastases with natural histories as indicated. Box plots depict the upper and lower quartiles, with the mean shown as a solid line; whiskers indicate the 1.5 times interquartile range (IQR). All data points are shown.

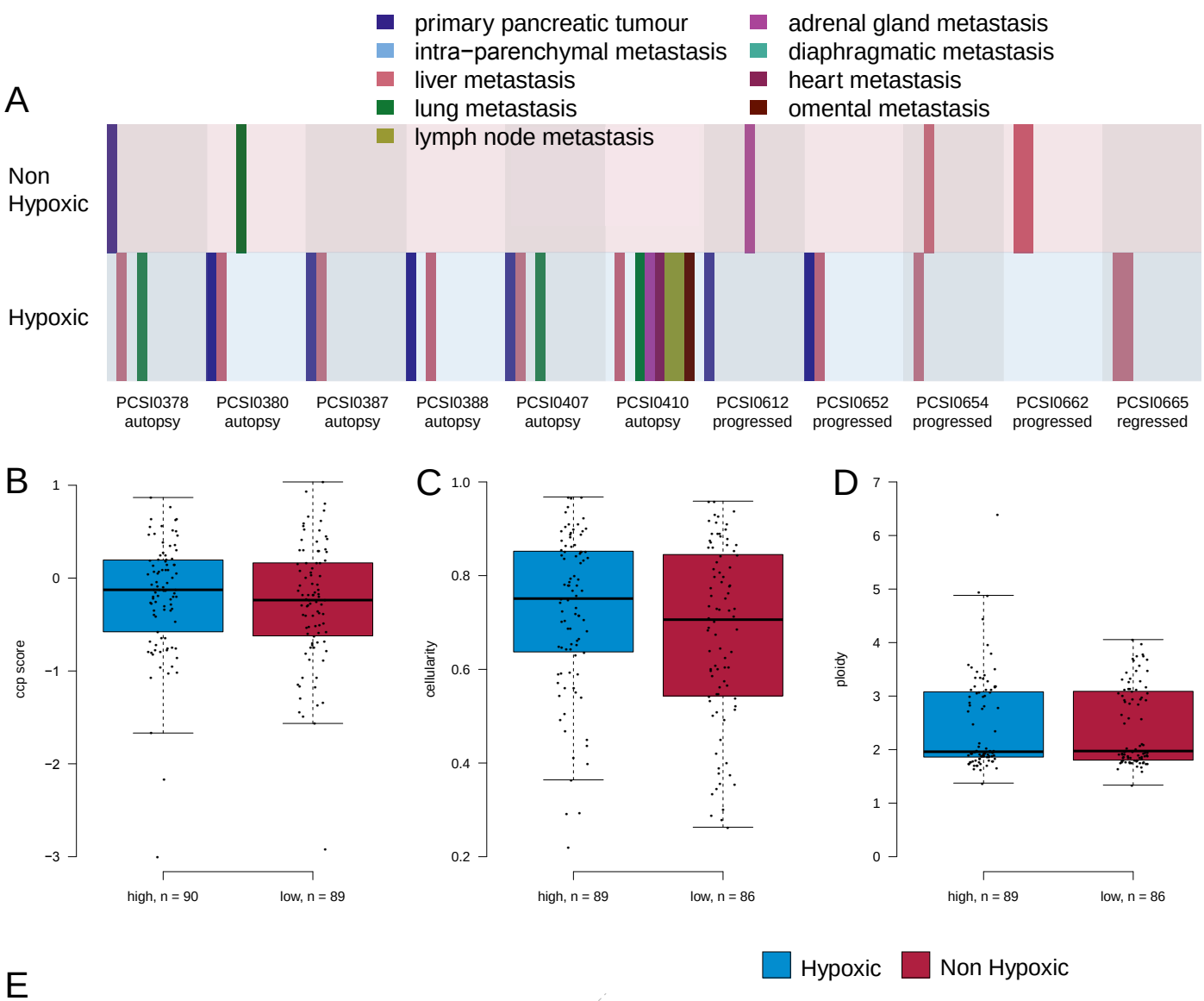

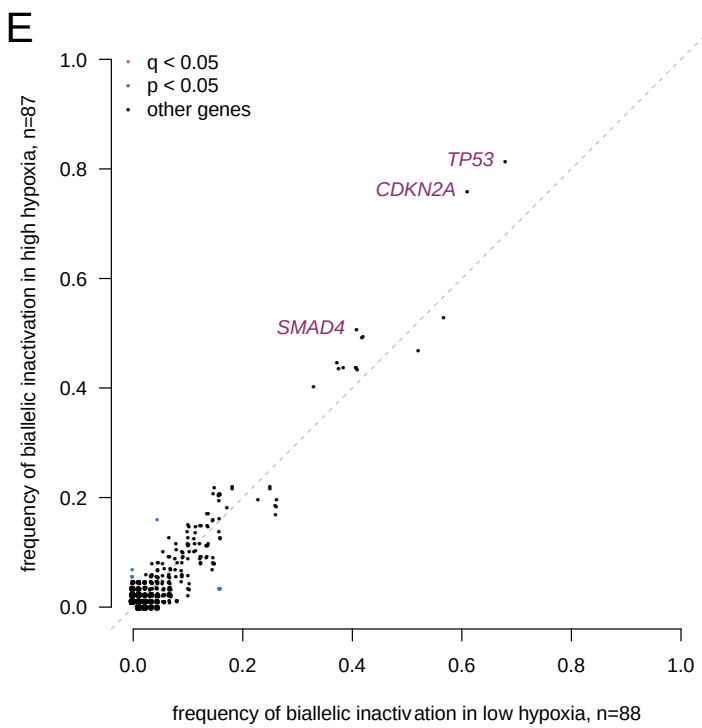

Figure S4: Related to Figure 3. (A) Gene expression based hypoxia score in paired primaries and metastases. (B-D) Boxplots show samples stratified by hypoxia with cell cycle progression scores (Kruskal-Wallis test p value: 0.317) (B), cellularity (Kruskal-Wallis test p value: 0.214) (C) and ploidy (Kruskal-Wallis test p value: 1.000) (D). (E) Frequencies of bi-allelic gene inactivation in unpaired primaries with high (y-axis) against low (x-axis) hypoxia. Box plots depict the upper and lower quartiles, with the mean shown as a solid line; whiskers indicate the 1.5 times interquartile range (IQR). Data points outside the IQR are shown.

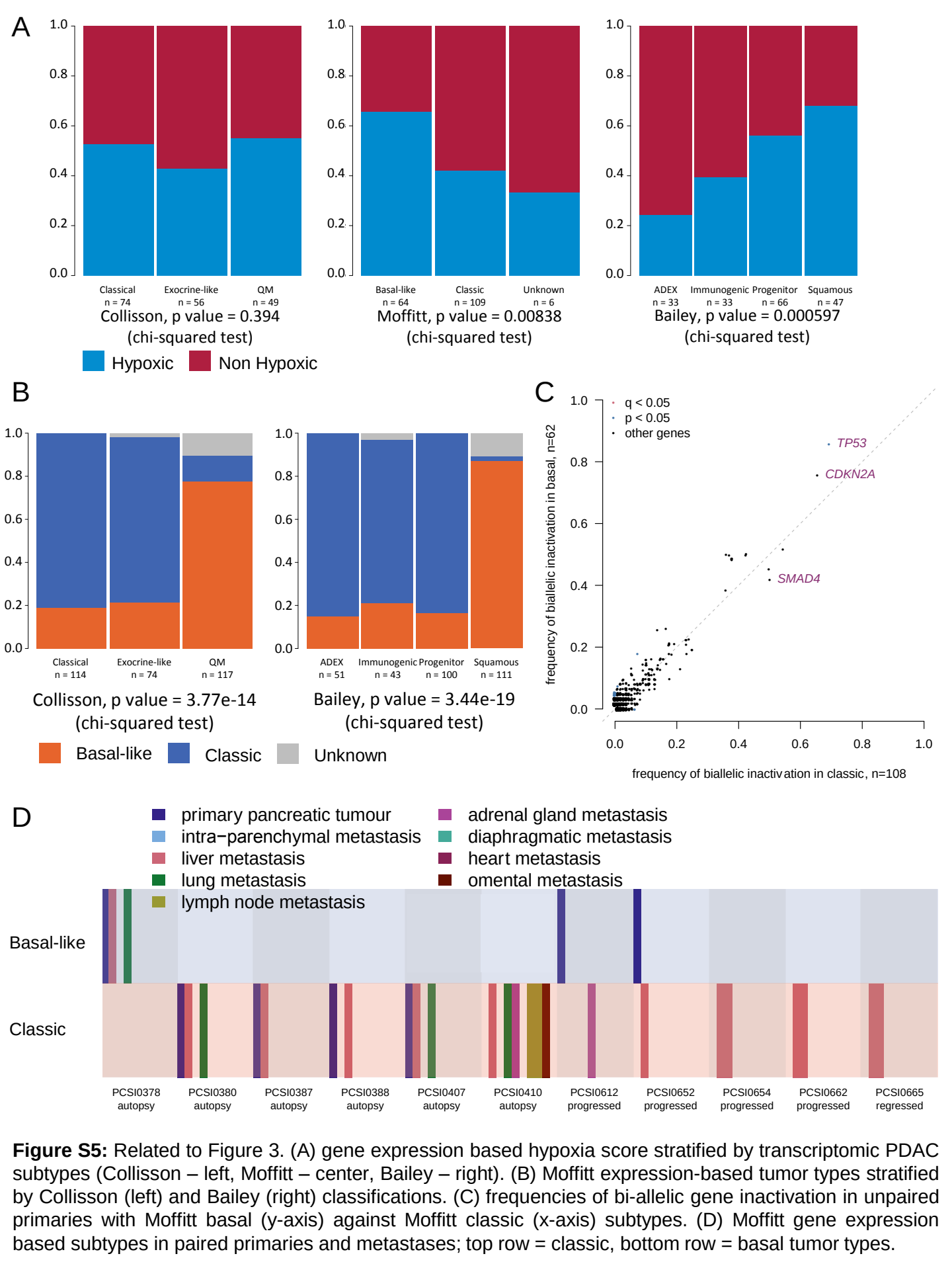

Figure S5: Related to Figure 3. (A) gene expression based hypoxia score stratified by transcriptomic PDAC subtypes (Collisson – left, Moffitt – center, Bailey – right). (B) Moffitt expression-based tumor types stratified by Collisson (left) and Bailey (right) classifications. (C) frequencies of bi-allelic gene inactivation in unpaired primaries with Moffitt basal (y-axis) against Moffitt classic (x-axis) subtypes. (D) Moffitt gene expression based subtypes in paired primaries and metastases; top row = classic, bottom row = basal tumor types.

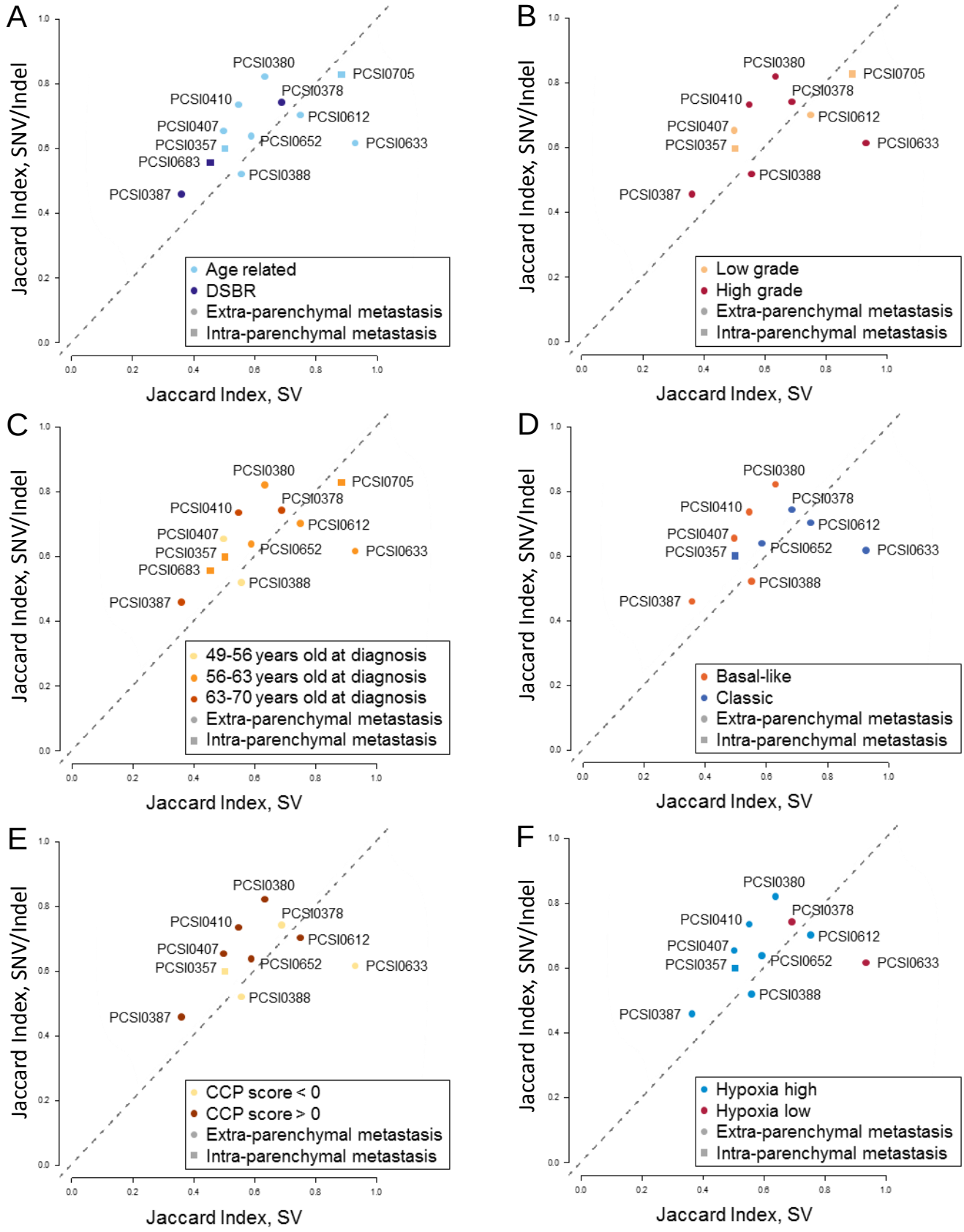

Figure S6: Related to Figure 6. (A-F) Scatterplots of Jaccard Indices for average simple (y-axis) and structural (x-axis) variation for each tumor pair. Points are colored by mutational signature (A), tumour grade (B), age at diagnosis (C), Moffitt class (D), CCP score (E) and hypoxia (F).

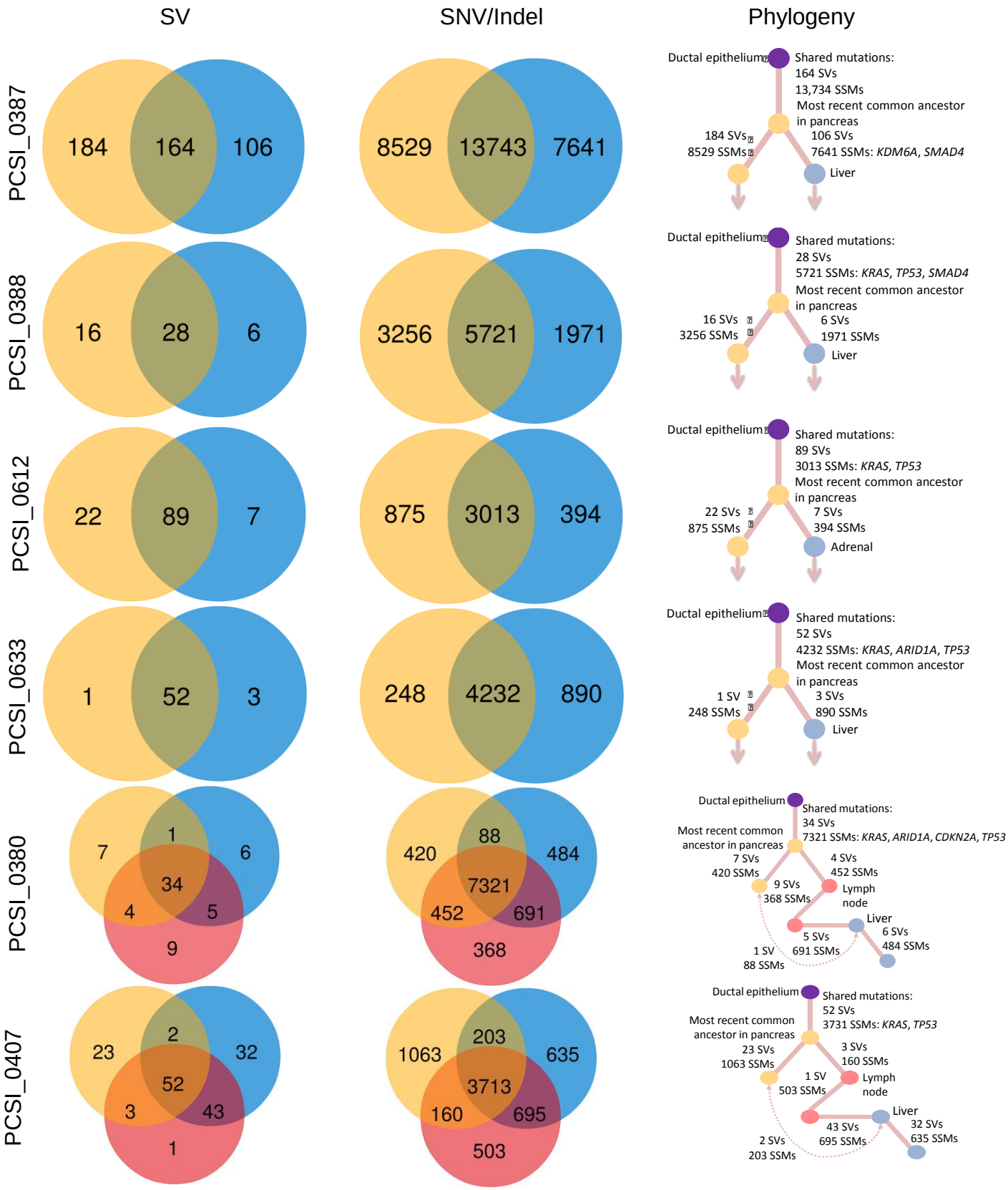

Figure S7: Related to Figure 6. 6 paired cases with Venn diagrams showing shared burden of SVs and SNVs/indels with inferred phylogenies.

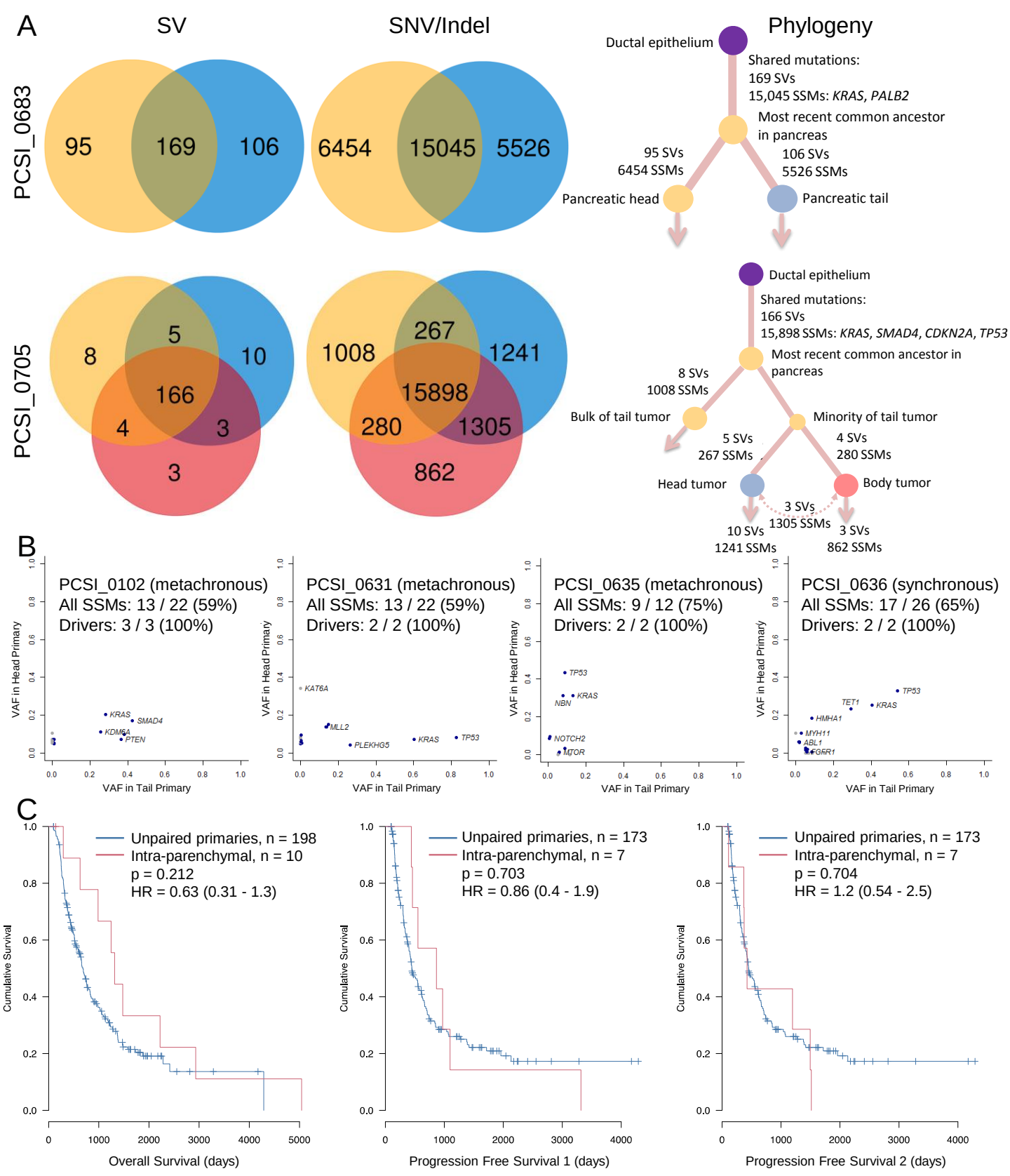

Figure S8: Related to Figure 7. (A) Venn diagrams showing shared burden of SVs and SNVs/indels with inferred phylogenies for two 'synchronous' cases. (B) Allele frequency plots of paired tumors from 3 additional metachronous and 1 additional synchronous case. (C) Overall survival (OS) (left) and progression free survival (PFS) (middle and right) for cases with intra-parenchymal recurrences compared to unpaired primaries. OS includes synchronous and metachronous cases. PFS1 & PFS2 include only the latter. PFS1 refers to the time from first resection to intra-parenchymal recurrence. PFS2 refers to time from second resection to further recurrence.

Table S4, related to Figure 8: Uni- and multi-variate overall survival analysis

Factor	number.0	number.1	p	p.fdr	HR	conf.int	multi.p.value.1	multi.HR.1	multi.lower.95.CI.1	multi.upper.95.CI.1	multi.p.value.2	multi.HR.2	multi.lower.95.CI.2	multi.upper.95.CI.2
Margin positivity (R1)	99	30	0.00322	0.0209	1.9	1.2-3.1	0.001	2.564	1.472	4.466	0.001	2.437	1.415	4.198
T stage (T1/T2 vs T3/T4)	18	115	0.0193	0.0502	2.1	1.1-4.1	0.014	2.507	1.207	5.208	0.026	2.294	1.104	4.765
Moffitt classification	73	46	0.0077	0.025	1.8	1.2-2.7	0.174	1.388	0.865	2.228	0.039	1.595	1.024	2.483
N stage (N0 vs N1)	28	104	3.32E-05	0.000432	3.3	1.8-5.9	0.041	2.145	1.031	4.460	0.048	1.917	1.007	3.651
TP53 biallelic inactivation	31	101	0.00726	0.025	2	1.2-3.3	0.049	1.881	1.002	3.529	0.056	1.764	0.985	3.161
Systemic therapy (neo & adj)	21	110	0.0277	0.0517	0.56	0.33-0.94	0.062	0.552	0.296	1.029	0.060	0.560	0.305	1.025
Hypoxia expression	57	64	0.0289	0.0517	1.6	1-2.4	0.218	1.341	0.841	2.139	NA	NA	NA	NA
Systemic therapy (adjuvant only)	24	107	0.0318	0.0517	0.58	0.35-0.96	NA	NA	NA	NA	NA	NA	NA	NA
Histology grade (well or moderate vs poor or undifferentiated)	97	32	0.315	0.407	1.3	0.81-2	0.960	1.015	0.576	1.788	NA	NA	NA	NA
SMAD4 biallelic inactivation	73	58	0.322	0.407	0.82	0.55-1.2	0.529	1.158	0.733	1.831	NA	NA	NA	NA
CDKN2 biallelic inactivation	36	95	0.344	0.407	1.2	0.79-2	0.701	0.895	0.509	1.575	NA	NA	NA	NA
CCP (divided by median CCP)	70	47	0.57	0.617	0.88	0.57-1.4	0.478	1.209	0.716	2.042	NA	NA	NA	NA
Systemic therapy (neoadjuvant only)	116	17	0.765	0.765	0.91	0.5-1.7	NA	NA	NA	NA	NA	NA	NA	NA

Table S5, related to Figure 8: Uni- and multi-variate progression-free survival analysis

factor	number.0	number.1	p	p.fdr	HR	conf.int	multi.p.value.1	multi.HR.1	multi.lower.95.CI.1	multi.upper.95.CI.1	multi.p.value.2	multi.HR.2	multi.lower.95.CI.2	multi.upper.95.CI.2
N stage (N0 vs N1)	28	97	2.40E-05	0.000312	3.5	1.9-6.5	0.008	2.893	1.326	6.309	0.001	3.106	1.636	5.896
Moffitt classification	68	48	0.0094	0.0306	1.8	1.1-2.8	0.146	1.443	0.881	2.365	0.027	1.629	1.056	2.513
TP53 biallelic Inactivation	30	92	0.00113	0.00734	2.5	1.4-4.3	0.029	2.097	1.078	4.079	0.140	1.508	0.874	2.603
CDKN2A biallelic inactivation	33	90	0.00495	0.0214	2.2	1.2-3.8	0.130	1.699	0.855	3.373	0.778	0.931	0.564	1.535
Hypoxia expression	57	63	0.0528	0.137	1.5	0.99-2.4	0.440	1.208	0.748	1.952	NA	NA	NA	NA
Systemic therapy (adjuvant only)	23	99	0.0846	0.173	0.61	0.34-1.1	NA	NA	NA	NA	NA	NA	NA	NA
Margin positivity (R1)	98	27	0.0934	0.173	1.6	0.92-2.6	0.233	1.442	0.791	2.628	NA	NA	NA	NA
T stage (T1/T2 vs T3/T4)	18	105	0.117	0.19	1.6	0.88-3.1	0.200	1.598	0.780	3.272	NA	NA	NA	NA
Systemic therapy (neo & adj)	20	102	0.175	0.253	0.65	0.34-1.2	0.098	0.557	0.279	1.114	NA	NA	NA	NA
SMAD4 biallelic inactivation	71	55	0.217	0.282	0.77	0.5-1.2	0.741	1.085	0.669	1.759	NA	NA	NA	NA
Systemic therapy (neoadjuvant only)	110	15	0.344	0.407	1.3	0.74-2.4	NA	NA	NA	NA	NA	NA	NA	NA
Histology grade	90	30	0.522	0.566	1.2	0.72-1.9	0.552	1.187	0.674	2.091	NA	NA	NA	NA
CCP (divided by median CCP)	69	49	0.963	0.963	0.99	0.63-1.5	0.428	1.241	0.728	2.115	NA	NA	NA	NA